RADIAL VELOCITIES AND THE HUBBLE LAW

Carrera Ortiz, School of Physics, Georgia Tech

ABSTRACT

In this report, there are two main objectives. First, we will analyze the spectral data of two galaxies and deduce their radial velocities given its central wavelengths. Then, we will analyze distance-radial velocity relationships of four categories of stellar objects (Cepheids, Tully-Fisher, Type Ia Supernovae, and Surface Brightness Fluctuations [SBF]) and determine the Hubble constant for each category, ultimately drawing comparisons between the 4.

1. AN INTRODUCTION

In order to determine how our Universe will end, if it will at all, we need to know what it is doing now. Is the universe collapsing on itself? Is it expanding? Edwin Hubble was able to answer this question by graphing the distance and radial velocities of galaxies and noticing a linear relationship that indicated that the universe was expanding. Though there is some expected error to this value, it is a crucial element of cosmology.

From what we know in the write-up, "The Hubble Constant is usually expressed in units of kilometers per second per megaparsec and sets the cosmic distance scale for the present Universe. The inverse of the Hubble Constant has dimensions of time. Locally, the Hubble Law relates the distance to an object and its redshift: $cz = Ho * d$, where d is the distance to the object and z is its redshift."

2. RADIAL VELOCITIES

We begin with the two galaxies NGC 4258 and NGC 3627. The provided spectral data is a set of the wavelength and its intensity, both under a 'blue' and 'red' spectrum, containing either the H_α or the H_β emission line.

The analysis starts by simply graphing the data given to notice the peaks, either 2 or 3 shown depending on which spectral data is being observed. Note that the 'red' spectra has 3 peaks, one of which contains H_α, while the 'blue' spectra has 2 peaks. For NGC 4258, the red spectra is graphed as shown in Table 2, and its blue counterpart shown in Table 1.

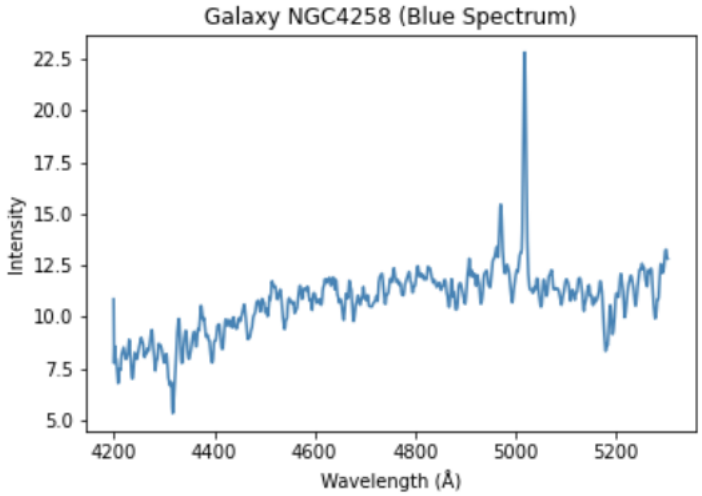

Figure 1. Initial graph of the blue spectral data from NGC 4258

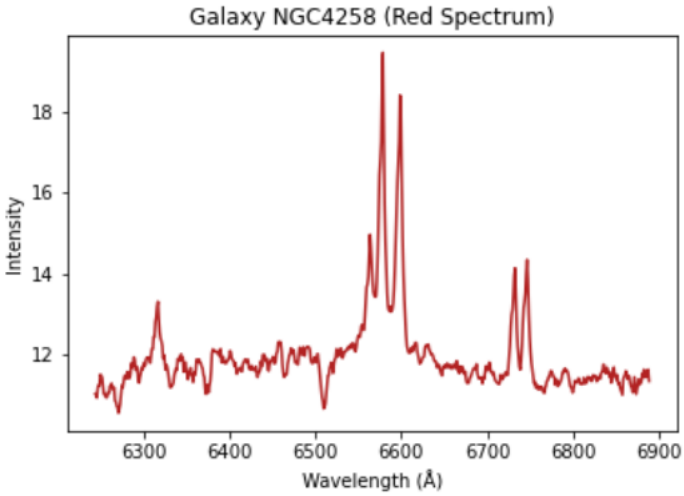

Figure 2. Initial graph of the red spectral data from NGC 4258

Moving on, we want to characterize and pinpoint the peaks shown in Tables 1 and 2. Thus, we apply a Gaussian fit in order to determine the central wavelengths. You can see the effect

of this process in Figure 3 as the peaks are highlighted between their general values below and above the peak, which can be increasingly narrowed down. This is repeated for each spectra of each galaxy. Note for later that the wavelength found in this process is absolutely critical.

In order to calculate the radial velocity for these galaxies, we use the relation:

$$v = (\frac{\lambda_{obs} - \lambda_0}{\lambda_0})c \tag{1}$$

Thus, the wavelength found as mentioned becomes our observed wavelength, while we reference known wavelengths for the emission spectra. The ultimate calculations for NGC 4258 are shown in Table 1.

The process is then repeated for each spectra in the other galaxy.

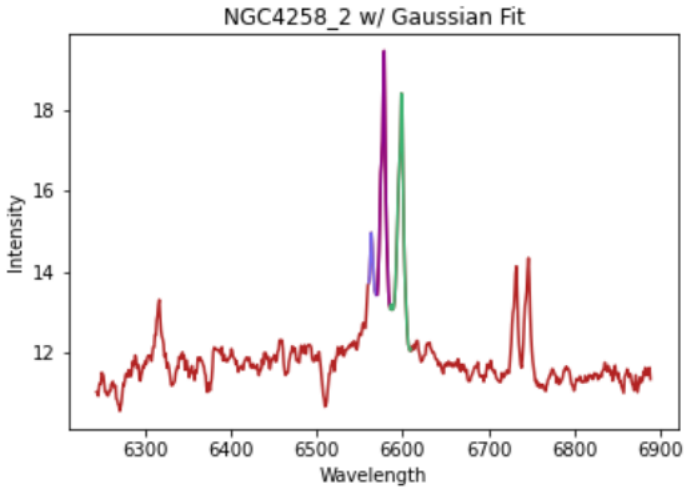

Figure 3. Gaussian Fit applied to Figure 2

Table 1. NGC 4258 Radial Velocity Data

Emission Line	Known Wavelength λ_o (Å)	Central Wavelength λ_{obs} (Å)	Radial Velocity (km/s)
O III	4958.911	4970.05	673.88
O III	5006.843	5017.98	667.31
N II	6548.050	6563.5	707.84
Hα	6562.819	6578.48	715.90
N II	6583.460	6598.45	683.08

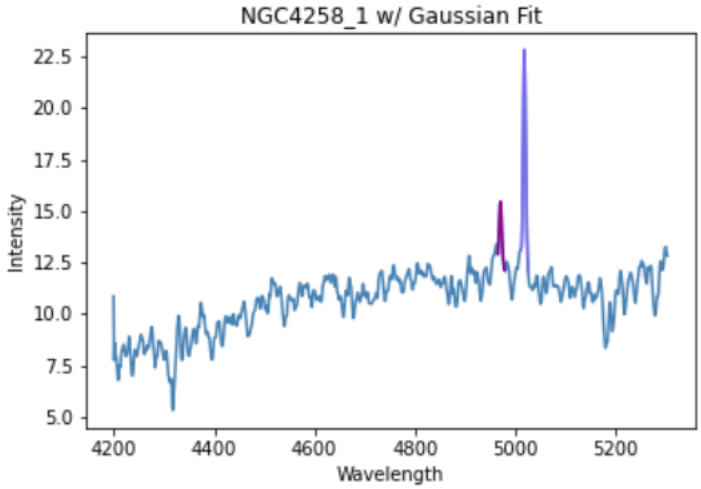

Figure 4. Gaussian Fit applied to Figure 1

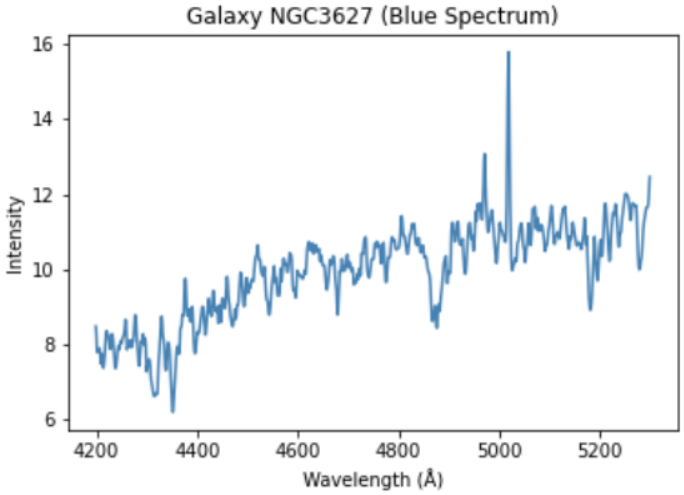

Figure 5. Initial graph of the blue spectral data from NGC 3627

The graphs for the spectral data of NGC 3627, with the same process as before, are shown below.

Table 2. NGC 3627 Radial Velocity Data

Emission Line	Known Wavelength λ_o (Å)	Central Wavelength λ_{obs} (Å)	Radial Velocity (km/s)
O III	4958.911	4970.86	712.84
O III	5006.843	5018.74	722.88
N II	6548.050	6563.13	709.96
Hα	6562.819	6578.09	698.07
N II	6583.460	6599.04	690.89

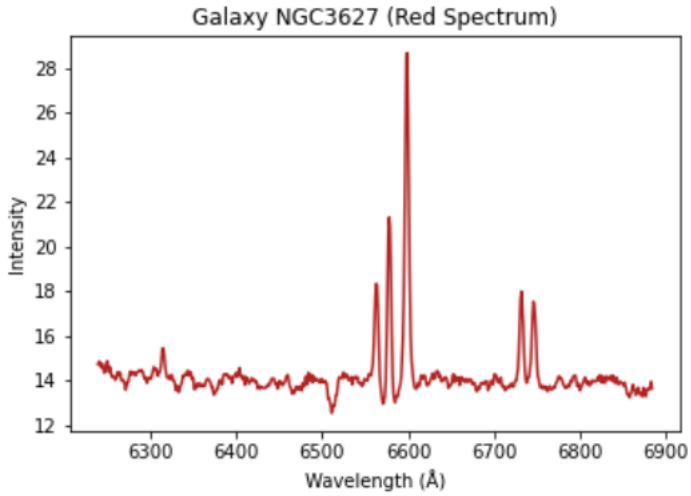

Figure 6. Initial graph of the blue spectral data from NGC 3627

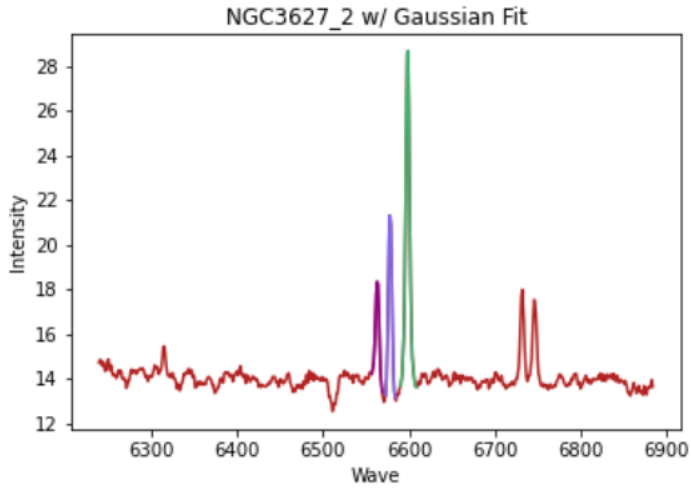

Figure 7. Gaussian Fit applied to Figure 6

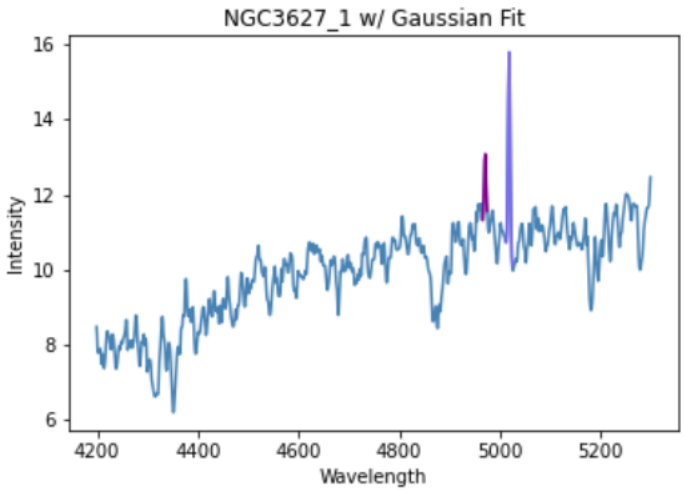

Figure 8. Gaussian Fit applied to Figure 5

3. DISTANCES – CEPHEIDS

Cepheids are interesting stellar objects largely due to the The Leavitt Law, discovered by Henrietta Leavitt. The Leavitt Law describes the period-luminosity relationship within Cepheids as they pulsate over a range of time. The consistency or lack there of is commonly used in reference with other objects. The Hubble Space Telescope observed many Cepheids, about 30 of which we will analyze in this report.

Thanks to authors listed at the end of the report, we are able to gather data that can be used in calculations to find the luminosity distance of each Cepheid. Additionally, NED from Caltech is utilized for radial velocity measurements, whose error bars ideally would be graphed (but wasn't working very well in python for me this time). These calculations alongside each noted Cluster that the Cepheid is found in are listed in Table 3.

Regarding the Cepheid data, not all was relevant for this report's purpose. First of all, some data did not have all relevant values, and others included a negative radial velocity, meaning that it was moving towards us, which is not useful in determining the recession of galaxies. For the cepheids, there is much less of a strong fit for the data, there is still a generally increasing nature to the plot shown in Figure 9.

The plot shows the relation mentioned in the introduction, whose slope is equivalent to the Hubble constant. I would like to note that I used two methods to calculate the Hubble constant, and they are not equivalent. The first method is from the linear regression calculation (in python). I assume that part of the reason this method is different is because it assumes that there is a valid y-intercept, which is not the case when calculating the Hubble constant.

The next is through the equation:

Table 3. Cepheid Data

Cluster	Distance (Mpc)	Radial Velocity (km/s)	$\sigma_{RV}(km/s)$
NGC 224	1.01	- 582	20
NGC 300	2.09	- 91	16
NGC 598	1.10	- 460	20
NGC 925	11.64	326	16
NGC 1326A	19.14	1725	8
NGC 1365	21.78	1539	7
NGC 1425	25.24	1412	7
NGC 2090	13.87	994	5
NGC 2541	14.06	687	10
NGC 3031	4.41	43	6
NGC 3198	16.14	879	15
NGC 3319	15.49	981	17
NGC 3351	12.19	1128	24
NGC 3368	12.25	1237	24
NGC 3621	9.86	1064	23
NGC 3627	12.25	1070	24
NGC 4258	9.95	667	14
NGC 4321	18.28	1896	23
NGC 4414	19.77	983	19
NGC 4496 A	16.90	2072	24
NGC 4535	18.37	2299	23
NGC 4536	17.70	2151	24
NGC 4548	18.20	808	23
NGC4639	24.66	1338	23
NGC 4725	16.44	1492	20
NGC 5253	3.99	681	19
NGC 5457	7.80	362	9
NGC 7331	19.23	490	23
IC 4182	4.72	550	16
IC 1613	0.77	- 560	23

$$H_0 = \frac{\Sigma(D_i V_i)}{\Sigma(D_i^2)} \tag{2}$$

Equation 2 is what is referenced on each Hubble Plot in this report. For the Cepheids, $H_0 \approx 73$ ((km/s) / Mpc).

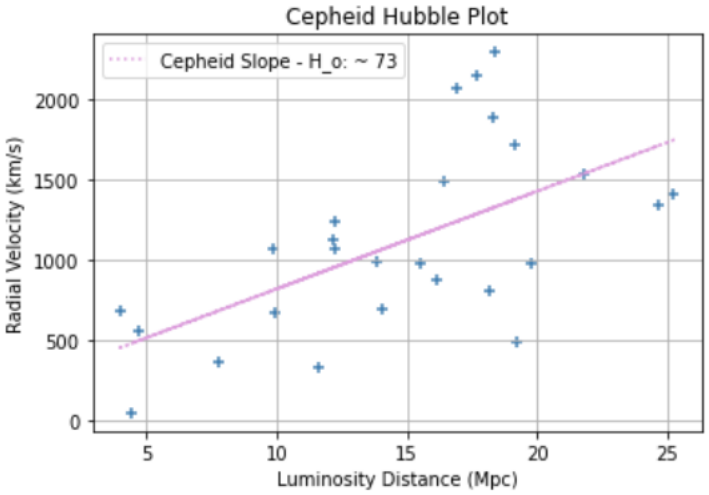

Figure 9. Cepheid Hubble Plot to Determine H_0

4. DISTANCES – SURFACE BRIGHTNESS FLUCTUATIONS

It is known that galaxies appear in some typical shapes, also described by Hubble (and others). For galaxies categorized as elliptical or early-spirals with a large bulge, it is possible to utilize the red giant branch luminosity function on the Population II red giant stars located within these galaxies. By the nature of the function, the magnitudes (μ) derived can be assumed to be universal and thus accurately derive distances using the formula:

$$\mu = m - M = 5log\frac{d_L}{10} \tag{3}$$

Which is then solved for distance and multiplied by a factor of a millionth in order to convert the distance into megaparsecs.

$$d_L(Mpc) = 10 * (10^{\mu/5}) * (0.000001) \tag{4}$$

The defining characteristics of each star is labeled in Table 4 below.

Again, we plot the calculated values and use Equation 2 to solve for the slope to ascertain the Hubble constant within the category of SBF. The Hubble Plot for SBF is shown in Figure 10

Table 4. Surface Brightness Fluctuations Data

Cluster	Distance (Mpc)	Radial Velocity (km/s)	$\sigma_{RV}(km/s)$
NGC 524	24.22	2092	22
NGC 4526	18.37	953	24
NGC 1404	20.19	1855	8
NGC 4424	15.99	774	24
NGC 1316	20.80	1694	8
NGC 1201	20.57	1531	16
NGC 524	24.22	2092	22
NGC 7619	52.05	3391	26
NGC 4763	24.20	4375	25
NGC 4386	27.42	1721	27
NGC 5839	22.25	1412	14
NGC 4125	24.23	1390	16
NGC 1316	20.80	1694	8
NGC 1380	21.20	1781	14
NGC 3923	22.48	2079	25
NGC 1404	20.19	1855	8
NGC 1316	20.80	1694	8
NGC 2258	50.12	4055	36
NGC 2962	33.11	2301	24
NGC 5061	28.31	2383	28
NGC 6495	41.69	3049	14
NGC 474	32.15	2001	23
NGC 4636	14.66	1275	24

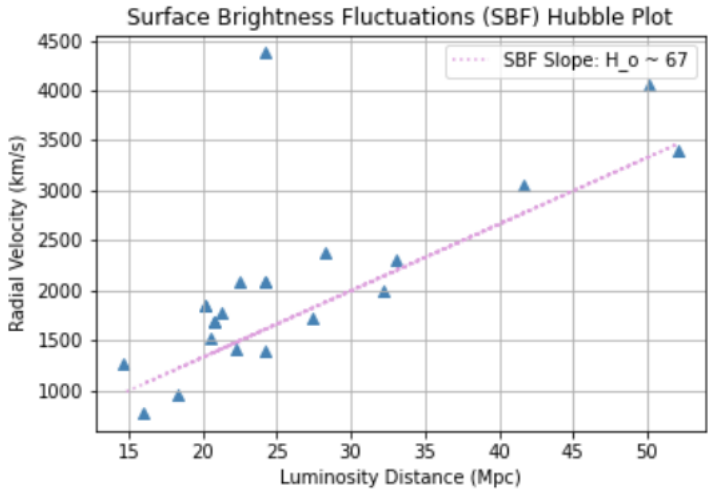

Figure 10. SBF Hubble Plot to Determine H_0

5. DISTANCES – TULLY-FISHER

Another option to obtain galactic distances is through the Tully-Fisher relationship, calibrated by the Leavitt Law which was previously discussed. Using this method, we are able to utilize the luminosity and maximum galactic rotation to determine the distances of galaxies. We then apply this relationship to the Hubble plots after collecting the distance and radial velocity data from Freedman et al. (2001). Note, all data is calibrated to the Cosmic Microwave Background.

The data representing Figure 11 is shown in Table 5.

Table 5. Tully-Fisher Data

Cluster	Distance (Mpc)	Rad. Velocity (km/s)
Abell 1367	89.2	6709
Abell 0262	66.7	4730
Abell 3574	62.2	4749
Abell 0400	88.4	7016
Antlia	45.1	3106
Cancer	74.3	4982
Cen 30	43.2	3272
Cen 45	68.2	4820
Coma	85.6	7143
Eridanus	20.7	1607
ESO 50	39.5	3149
Fornax	15.0	1380
Hydra	58.3	4061
MDL 59	31.3	2304
NGC 3557	38.7	3294
NGC 0383	66.6	4924
NGC 0507	57.3	4869
Pavo 2	50.9	4398
Pegasus	53.3	3545
Ursa Major	19.8	1088

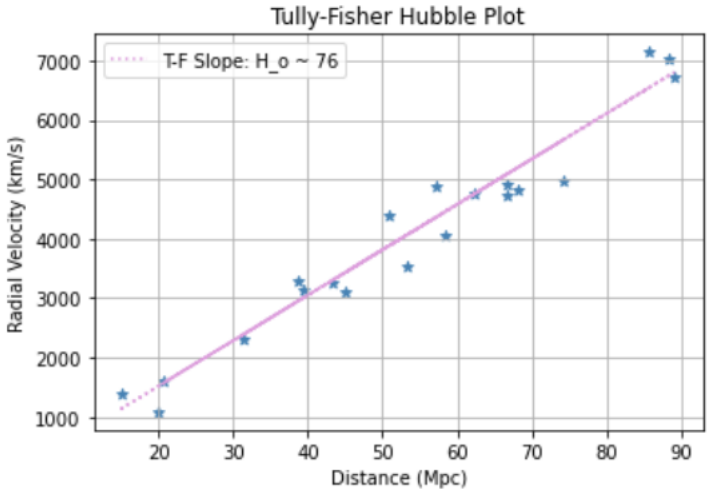

Figure 11. Tully-Fisher Plot to Determine H_0

6. DISTANCES – TYPE IA SUPERNOVAE

It is an astronomer's dream to view a supernovae explode during their lifetime. These intensely bright phenomena provide a very accurate data point for calculating distances on the astronomical scale, allowing us to accurately see much farther. We continue to follow the pattern to yield the tabulated data used to form the Figure 12.

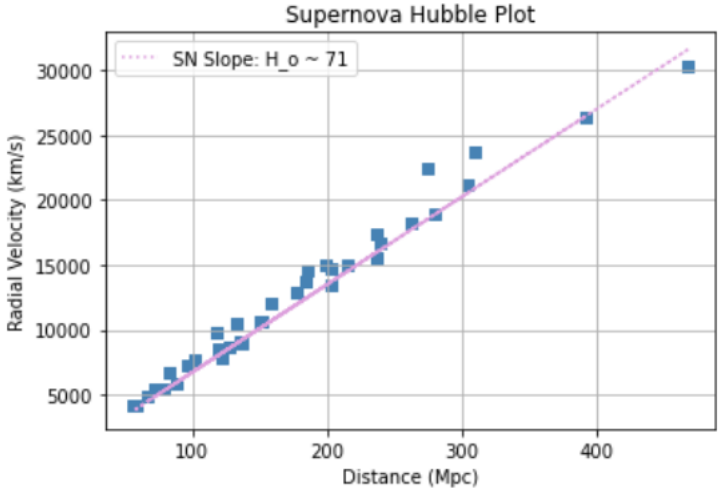

Figure 12. Supernovae Hubble Plot to Determine H_0

Table 6. Type Ia Supernovae Data

Cluster	Distance (Mpc)	Radial Velocity (km/s)
SN1990O	134.7	9065
SN1990T	158.9	12012
SN1990af	198.6	15055
SN1991S	238.9	16687
SN1991U	117.1	9801
SN1991ag	56.0	4124
SN1992J	183.9	13707
SN1992P	121.5	7880
SN1992ae	274.6	22426
SN1992ag	102.1	7765
SN1992al	58.0	4227
SN1992aq	467.0	30253
SN1992au	262.2	18212
SN1992bc	88.6	5935
SN1992bg	151.4	10696
SN1992bh	202.5	13518
SN1992bk	235.9	17371
SN1992BL	176.8	12871
SN1992bo	77.9	5434
SN1992bp	309.5	23646
SN1992br	391.5	26318
SN1992bs	280.1	18997
SN1993B	303.4	21190
SN1993O	236.1	15567
SN1993ag	215.4	15002
SN1993ah	119.7	8604
SN1993ac	202.3	14764
SN1993ae	71.8	5424
SN1994M	96.7	7241
SN1994Q	127.8	8691
SN1994S	66.8	4847
SN1994T	149.9	10715
SN1995ac	185.6	14634
SN1995ak	82.4	6673
SN1996C	136.0	9024
SN1996bl	132.7	10446

7. DISTANCES – COMBINED DATA

In this combined set, I not only entered all the data from previous plots, but an additional 'odd' data point from the Tully-Fisher set that although was far from the other objects in its

set is not as much of an outlier with the distances extended out from the Type Ia Supernovae data. Ultimately the Hubble constant overall is calculated to be ≈ 71, which is an often used value in cosmology (69-72 is what I've most commonly seen used, most often simplified to 70). Though some values for H_0 can be high for a certain category, the overall relationship matches our current understanding from Hubble, who seems to be rightfully dedicated in astronomical history for his discovery.

Table 7. Combined Hubble Data

Category	# of Obj. in Category	Hubble Constant ((km/s)/Mpc)
Cepheid	30	73
Surface Brightness Fluctuations	23	78
Tully-Fisher	21	76
Type Ia Supernovae	36	71

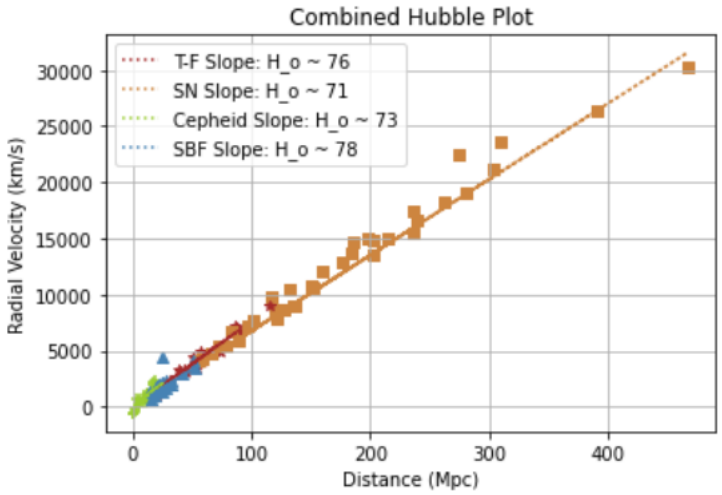

Figure 13. Combined Plot showing the continuous nature of the Hubble Constant at Large Distances

8. SUMMARY

Though there are significant differences in each category's Hubble constant (78 being quite a large especially), I am very satisfied that the ultimate calculation at the end was well within a decent margin of error for the known value. I think that a large reason for this is the impact of the very accurate supernovae that provide a precise method for calculating distance and therefore a more accurate graph of Hubble's Law. It then tracks that less precise methods, such as the use of Surface Brightness Fluctuations, is less accurate to the data when it requires many assumptions to be used. Additionally, a large portion of the data provided for this included error bars, which were not included in this report, but would be incredibly useful in determining the likelihood of the most accurate value for the Hubble constant.

9. WORKS CITED

Freedman, W. L. et al., Astrophysical Journal, 553, 47, 2001

Freedman, W. L. & Madore, B. F., Annual Reviews of Astronomy and Astrophysics, 48, 673, 2010

Ho, L. C., Filippenko, A. V., & Sargent, W. L. W., Astrophysical Journal, 98, 477, 1995

Hubble E. P., Proc. Natl. Acad. Sci. USA 15, 168, 1929

Khetan, N. et al., Astronomy and Astrophysics, 647, A72, 2021

Leavitt H. S., Ann. Harv. Coll. Obs. 60, 87, 1908

Lemaitre G., Ann. Soc. Sci. Brux. 47, 49, 1927

http://ned.ipac.caltech.edu